

Cross-Modal Retrieval Meets Inference: Improving Zero-Shot Classification with Cross-Modal Retrieval

Seongha Eom¹, Namgyu Ho¹, Jaehoon Oh^{2*}, Se-Young Yun^{1*}

¹Graduate School of AI, KAIST

²Samsung Advanced Institute of Technology
{doubleb, itsnamgyu, yunseyoung}@kaist.ac.kr, jh0104.oh@gmail.com

Abstract

Contrastive language-image pre-training (CLIP) has demonstrated remarkable zero-shot classification ability, namely image classification using novel text labels. Existing works have attempted to enhance CLIP by fine-tuning on downstream tasks, but these have inadvertently led to performance degradation on unseen classes, thus harming zero-shot generalization. This paper aims to address this challenge by leveraging readily available image-text pairs from an external dataset for cross-modal guidance *during inference*. To this end, we propose X-MoRe, a novel inference method comprising two key steps: (1) cross-modal retrieval and (2) modal-confidence-based ensemble. Given a query image, we harness the power of CLIP’s cross-modal representations to retrieve relevant textual information from an external image-text pair dataset. Then, we assign higher weights to the more reliable modality between the original query image and retrieved text, contributing to the final prediction. X-MoRe demonstrates robust performance across a diverse set of tasks without the need for additional training, showcasing the effectiveness of utilizing cross-modal features to maximize CLIP’s zero-shot ability.

1 Introduction

Pre-trained vision-language models, such as Contrastive Language-Image Pre-training (CLIP) (Radford et al. 2021), have demonstrated their effectiveness in acquiring transferable features from paired image and text data. The training process of CLIP harnesses two scalable elements: data and computational power. Firstly, the abundance of extensive image-text pairs available for training greatly contributes to its comprehensive learning. Secondly, CLIP’s utilization of co-embeddings for images and language allows it to efficiently scale with computational resources. Consequently, CLIP has served as an alternative pre-training method, often replacing other visual pre-training approaches such as SimCLR (Chen et al. 2020) or MAE (Masked Autoencoder) (He et al. 2022) across a wide range of applications. Subsequent techniques built upon language-image pre-training, like FLIP (Li et al. 2023), Audioclip (Guzhov et al. 2022) and Videoclip (Xu et al. 2021), also show comparable favorable scaling results.

CLIP has been demonstrated to learn visual-language representations with substantial potential in zero-shot classification

tasks. In order to enhance its effectiveness in downstream tasks, recent research studies have proposed the incorporation of additional learnable elements into CLIP, accompanied by adjustments made through the utilization of few-shot training datasets. Zhou et al. (2022a,b) implement prompt tuning, while Zhang et al. (2021) introduce adapters inspired by large language models. As a result, CLIP’s pre-trained weights are kept fixed; instead, adaptable inputs or lightweight adapters are introduced to fine-tune textual or visual features.

Even though the inclusion of learnable inputs (Zhou et al. 2022a,b) or adapters (Zhang et al. 2021) demonstrates remarkable enhancements when dealing with seen classes during fine-tuning, their zero-shot performance on unseen classes tends to diminish. Thus, recent studies have indicated that these learnable inputs, specifically prompts, can be effectively tuned for a query image *during inference*, eliminating the requirement for fine-tuning CLIP (Shu et al. 2022; Gao et al. 2022). Meanwhile, Guo et al. (2023) proposed using intermediate visual and textual features instead of learnable parameters for zero-shot enhancement of CLIP.

In addition, while these endeavors concentrate on leveraging visual input data to make well-founded model decisions, it is worth noting that the role of the language modality remain relatively unexplored for zero-shot classification. For instance, the text encoder within CLIP has been validated as beneficial for enhancing tasks in relation to other modalities (Chen et al. 2023). Kim, Kwon, and Ye (2022) proved that text guidance from CLIP can give support for image generation task. Menon and Vondrick (2022) showed that visual descriptions of each category, instead of name, is helpful for explainable image classification task.

Therefore, to leverage the potential of the text modality during inference, we propose a novel *tuning-free inference* method while preserving CLIP’s zero-shot ability, called X-MoRe (**Cross-Modal Retrieval based Inference**). Our method, illustrated in Figure 1, is composed of two key steps: (1) cross-modal retrieval and (2) modal-confidence-based ensemble. In the cross-modal retrieval step, we create a pool of image-text pairs from an external dataset based on the similarity between a query image and images. We then meticulously retrieve texts from this pool of image-text pairs based on the direct similarity between a query image and texts. In the modal-confidence-based ensemble step, we

*Corresponding authors.

ensemble both the image-modal and text-modal predictions using modal-confidence weighting.

Our work can be summarized as follows:

- We propose $X\text{-MoRe}$, a novel tuning-free method for inference based on cross-modal retrieval. To capitalize on not only the image modality but also the text modality, $X\text{-MoRe}$ consists of cross-modal retrieval and modal-confidence-based ensemble steps (**Section 3**).
- We establish the superiority of our approach in zero-shot classification across 10 datasets and domain generalization tasks (**Section 4**). Furthermore, we conduct several ablation studies to investigate the effectiveness of individual components of $X\text{-MoRe}$ (**Section 5**).
- We analyze the confidence of the image and text modalities and demonstrate that the correct modality exhibits higher confidence. Specifically, when the prediction from the image is correct and the prediction from the text is incorrect, the image modality is given higher priority, and vice versa for the text modality (**Section 6**).

2 Related Work

2.1 Vision Language Model

Vision-Language Models (VLMs) are a class of models that integrate both visual and textual information to perform a wide range of tasks that require a deep understanding of both domains. Training VLMs typically involves contrastive learning, a self-supervised learning paradigm that encourages the model to learn representations by comparing positive and negative pairs. The objective of VLMs is to align image and text representations in a shared embedding space, such that semantically similar images and texts are brought closer together while dissimilar ones are pushed apart. Subsequently, to employ the trained model on downstream classification tasks, CLIP constructs the textual inputs by the category names and converts the original classification task into an image-text matching problem. Consequently, CLIP has demonstrated its capacity to execute zero-shot recognition in open-vocabulary scenarios, yielding encouraging results on a range of benchmarks.

Various approaches have been developed to improve the classification performance of VLMs. CLIP-Adapter (Gao et al. 2022) and Tip-Adapter (Zhang et al. 2021) use few-shot data to fine-tune lightweight adapters of CLIP on downstream tasks. Inspired by prefix-tuning methods from language models (Li and Liang 2021), Context Optimization (CoOp) (Zhou et al. 2022b) has initiated a line of work that aims to preserve the original model and optimize context embeddings, i.e. surrounding the class label. Recently, CALIP (Guo et al. 2023) introduced an approach that uses image-patchwise attention to enable fine-grained cross-modal alignment to enhance zero-shot classification in a parameter-free manner, extendable to few-shot settings.

2.2 Cross-modal Retrieval

Retrieval based module is also adopted for natural language generation in KNN-LM (Khandelwal et al. 2019) and image recognition in (Isken et al. 2023; Isken, Fathi, and Schmid

2023; Hu et al. 2023). Different from previous works which typically store features and label from models as key-value pair, we store image index and captions in natural language text as key-value pair which is much more lightweight. In another line of work, information is retrieved from knowledge graphs to improve the factuality of language models in applications such as dialogue and question answering (Kang et al. 2023; Baek, Aji, and Saffari 2023) or aid language models in tasks which require domain-specific knowledge (Kang, Baek, and Hwang 2022). Inspired by the success of knowledge fusion from cross-modal retrieval, we collect relevant captions for the query image by performing KNN search over an external image-text pair dataset.

2.3 Cross-modal Ensemble

Cross-modal ensembles have been employed to solve the multilingual video corpus moment retrieval (mVCMR) task (Liu et al. 2022; Lei, Berg, and Bansal 2021). This task involves retrieving short moments from a large corpus of videos with subtitles, given a natural language query, in various languages. mVCMR methods ensemble information from the subtitles and the visual content to determine the similarity of video moments to a given query. Meanwhile, recent work from the CLIP literature utilizes an ensemble of various visual information for test-time prompt-tuning (Shu et al. 2022). In particular, the prompt is optimized to perform consistently across multiple augmented views of each query image. To avoid noisy augmentations, the authors introduce confidence selection, which discards views with low-entropy class predictions. Our method can be seen as a form of cross-modal ensemble, utilizing information from the query image as well as retrieved captions. Inspired by Shu et al. (2022), we employ entropy to determine ensemble weights for each modality, to enhance the reliability of predictions.

3 X-MoRe: Cross-Modal Retrieval Inference

In this section, we propose $X\text{-MoRe}$, which is a novel inference method based on cross-modal retrieval and modal-confidence-based ensemble.

3.1 Prerequisite: CLIP Inference

CLIP comprises an image encoder, denoted as f , and a text encoder, denoted as g , as its core components. They respectively embed images and textual descriptions into high-dimensional representations. During CLIP training, it learns to align these image and text representations in a shared embedding space. When CLIP is applied to a zero-shot classification task, a query image X is embedded using f and the text labels with a pre-defined prompt (e.g., “a photo of a [CLS]”) are embedded using g . In the image-text embedding space, a query image has similarities measured with all of C text labels. Here, we define the *image-modal probability* $P_{img}(y|X)$ from the similarities. Then, a query image is predicted as the text label with the highest probability. This zero-shot classification inference is illustrated with a dotted gray line in Figure 1.

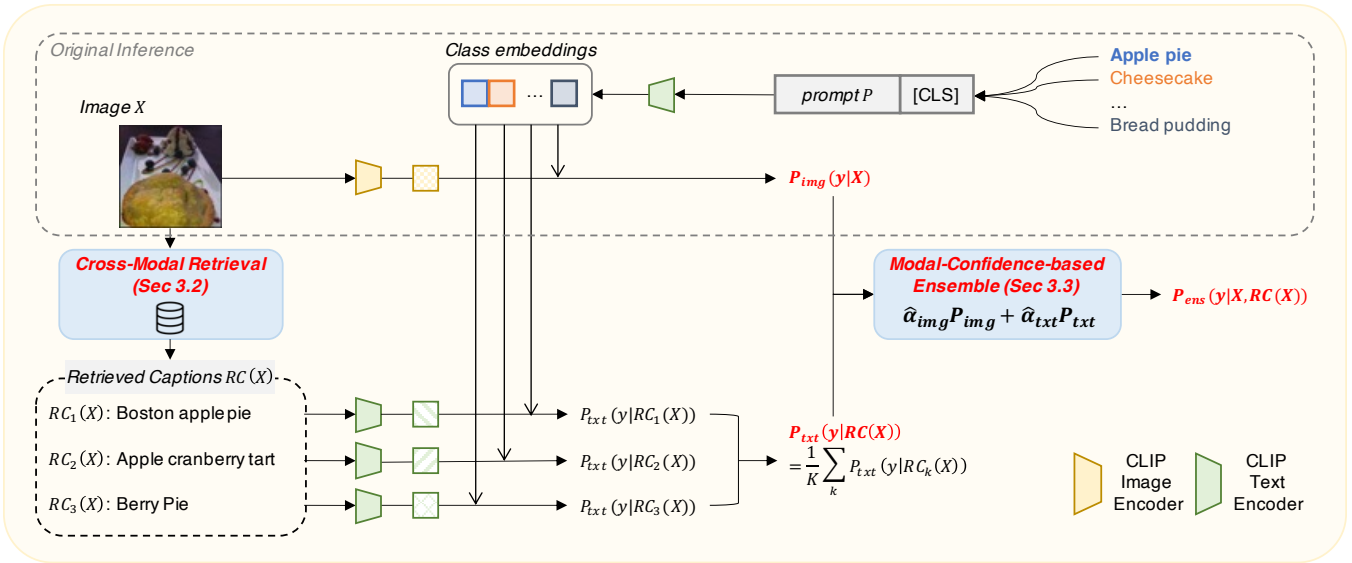


Figure 1: X-MoRe overview. Our pipeline first retrieves K (e.g., $K=3$ in this figure) captions from an external dataset in cross-modal manner (Section 3.2). Then, we ensemble the image-modal prediction $P_{img}(y|X)$ and the text-modal prediction $P_{txt}(y|RC(X))$ based on each modal-confidence (Section 3.3). Note that the original inference uses only image-modal prediction $P_{img}(y|X)$ as shown in grey dotted line.

3.2 Cross-modal Retrieval

We propose a two-step cross-modal retrieval method: image-based retrieval then text-based fine-retrieval. Figure 2 illustrates the retrieval process. Given a query image X , we coarsely obtain N images and corresponding texts based on the similarity between a query image X and the images from an external image-text dataset (e.g., public dataset or web-scale image-text database). Then, we finely obtain K texts based on the similarity between a query image X and texts from N image-text candidates. This stage is designed to be independent of inference, thereby reinforcing retrieval capabilities through the utilization of enhanced language-image pre-trained models.

STEP1. Image-based Retrieval We initially construct a set of N image-text candidates for a given query image X by focusing on the image modality. This is achieved through a KNN retrieval module, which searches the nearest neighbors from an external image-text dataset, following previous works (Isken, Fathi, and Schmid 2023; Isken et al. 2023; Hu et al. 2023; Khandelwal et al. 2019). For instance, Isken et al. (2023) employ the image modality to search the nearest neighbors and retrieve the corresponding texts from image-text pairs. The key difference from prior works is that we establish a set of N candidates larger than K , because the text modality is not directly considered within this step.

STEP2. Text-based Fine-retrieval In order to retrieve textual content associated with a query image X more accurately, we fine-retrieve K text captions $RC(X)$ from the pool of coarsely retrieved N image-text candidates. This procedure is important because there are cases where the

ranking of similarity between a query image X and images does not align with the ranking of similarity between the query image and their corresponding texts. Put simply, in the cross-modal embedding space, even if image X is closer to img_1 than to img_2 , it could be closer to txt_2 (the corresponding text of img_2) than to txt_1 (the corresponding text of img_1). Without this direct approach, it is hard to conceive that the retrieving texts used for predicting images are well describing the inputs.

After fine-retrieval, we define the *text-modal probability* $P_{txt}(y|RC(X))$ by averaging predictions obtained from the K retrieved captions $RC(X)$. This aggregation is utilized to create a single representative distribution for the text modality, thereby aligning it with the image-modal probability $P_{img}(y|X)$. Additionally, it prevents the text-modal probability from making overconfident incorrect predictions, which will be addressed in Section 6.1.

3.3 Modal-confidence-based Ensemble

After acquiring the image-modal probability $P_{img}(y|X)$ through the original inference and the text-modal probability $P_{txt}(y|RC(X))$ through the cross-modal retrieved inference, the two probabilities are ensemble based on modal-confidence for the *cross-modal probability* $P_{ens}(y|X, RC(X))$, which is the final prediction of X-MoRe.

For our modal-confidence, we contemplate a scenario where test images arrive sequentially, one by one. Indeed, when the test images come in a batch, if they are processed one by one, it is essentially similar to our scenario. Specifically, a query image X and retrieved captions $RC(X)$

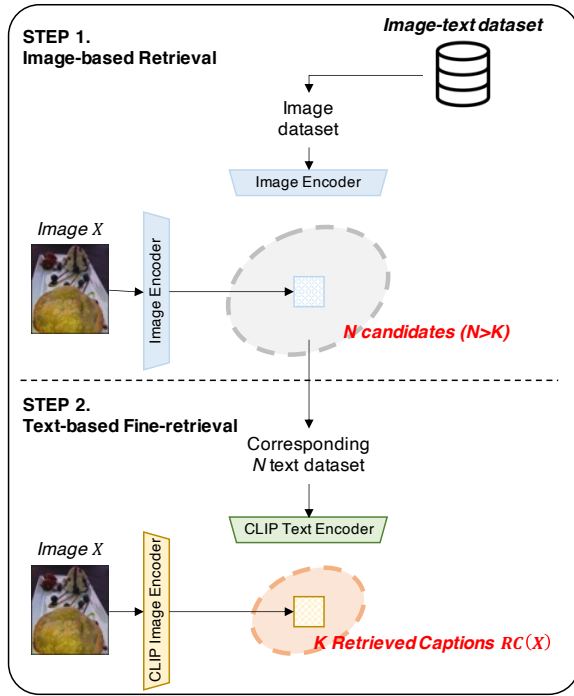


Figure 2: An overview of our two-stage cross-modal retrieval, starting with image-based retrieval and followed by text-based fine-retrieval. Given a query image X , we first obtain N image-text candidates from an external image-text dataset based on image similarity. This process is then refined to retrieve K texts by directly comparing the query image X to the texts of the N candidates.

at test time t is denoted as X^t and $RC(X^t)$. Then, for simplicity, we express $P_{img}(y|X^t)$, $P_{txt}(y|RC(X^t))$, and $P_{ens}(y|X^t, RC(X^t))$ as P_{img}^t , P_{txt}^t , and P_{ens}^t , respectively.

Image-confidence α_{img}^t and text-confidence α_{txt}^t at time t are fundamentally based on entropy as follows:

$$\alpha_{img}^t = 1 - \frac{H(P_{img}^t)}{H(P_{uni})}, \quad \alpha_{txt}^t = 1 - \frac{H(P_{txt}^t)}{H(P_{uni})} \quad (1)$$

where $H(\cdot)$ is the entropy of a probability distribution and P_{uni} is an uniform distribution over C classes (i.e., $[\frac{1}{C}, \dots, \frac{1}{C}]$). Modal-confidence values move closer to 0 when the probability distribution resembles a uniform distribution, whereas they move closer to 1 when the probability distribution concentrates on a specific class.

After calculating both confidence, we independently adjust them with min-max normalization within the confidences accumulated from previous test time. This is because the two different modalities have different entropy distributions. For instance, say that both of α_{img}^t and α_{txt}^t are 0.7. However, if the maximum value of α_{img} is 0.6 and the minimum value of α_{txt} is 0.8 until $t-1$, then X^t is the most confident image and $RC(X^t)$ is the least confident text. With this concern, adjusted image-confidence $\hat{\alpha}_{img}^t$ and adjusted text-confidence $\hat{\alpha}_{txt}^t$ are as follows, depicted in Figure 3:

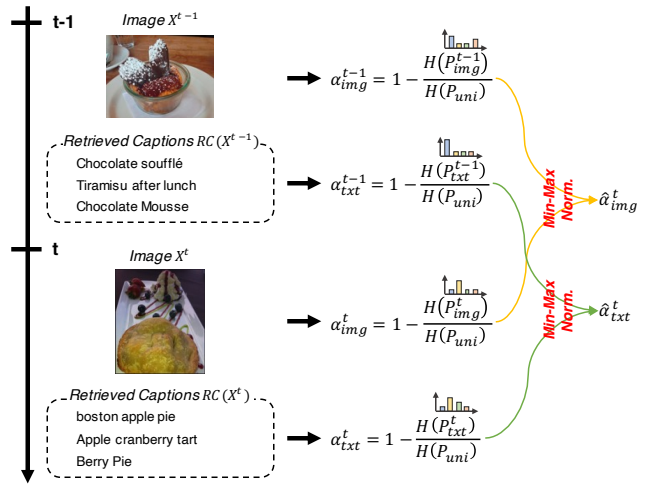


Figure 3: An example of calculating modal-confidences at time t . We first compute modal-confidences (i.e., α_{img}^t and α_{txt}^t) based on entropy of each prediction probability. Then, we independently calibrate these modal-confidences using min-max normalization, resulting in adjusted confidences (i.e., $\hat{\alpha}_{img}^t$ and $\hat{\alpha}_{txt}^t$), within the confidences encountered from previous test time.

$$\hat{\alpha}_{img}^t = \frac{\alpha_{img}^t - \min(\alpha_{img}^{1:t})}{\max(\alpha_{img}^{1:t}) - \min(\alpha_{img}^{1:t})} \quad (2)$$

$$\hat{\alpha}_{txt}^t = \frac{\alpha_{txt}^t - \min(\alpha_{txt}^{1:t})}{\max(\alpha_{txt}^{1:t}) - \min(\alpha_{txt}^{1:t})} \quad (3)$$

where $\min(\alpha^{1:t})$ and $\max(\alpha^{1:t})$ can be updated at each time t . With these adjusted modal-confidences, the cross-modal probability P_{ens}^t for the final prediction at test time t is calculated as follows:

$$P_{ens}^t = \hat{\alpha}_{img}^t P_{img}^t + \hat{\alpha}_{txt}^t P_{txt}^t \quad (4)$$

Our modal-confidence does not represent the directly relative confidence between the modalities, but rather it represents the relative confidence in each individual modality. It means that both $\hat{\alpha}_{img}^t$ and $\hat{\alpha}_{txt}^t$ independently take values between 0 and 1. For instance, if $\hat{\alpha}_{img}^t$ is 1, it means that the query image at time t has the highest confidence (i.e., lowest entropy) among the images encountered so far; conversely, if it is 0, it means that the query image at time t has the lowest confidence (i.e., highest entropy).

4 Experiment

4.1 Settings

We evaluate our approach using two types of CLIP models: CLIP-RN50 (f is ResNet50 (He et al. 2016) and g is 12-layer Transformer (Vaswani et al. 2017)) and CLIP-ViT-B/16 (f is ViT-B/16 (Dosovitskiy et al. 2020) and g is 12-layer Transformer (Vaswani et al. 2017)). During inference, we resize all test images to a resolution of 224×224 and employ the general textual template “a photo of a [CLS]”

Method	Flower102	DTD	Pets	Cars	UCF101	Caltech101	Food101	SUN397	Aircraft	EuroSAT	Avg.
CLIP-RN50 [†]	61.75	40.37	83.57	55.70	58.84	85.88	73.97	58.80	15.66	23.69	55.82
Caption Ensemble	59.36	35.40	62.74	43.82	51.44	81.82	70.00	49.44	19.50	29.65	50.32
CALIP	60.90	39.89	81.25	55.64	54.59	83.94	71.49	56.84	15.72	24.22	54.45
TPT [†]	62.69	40.84	84.49	58.46	60.82	87.02	74.88	61.46	17.58	28.33	57.66
X-MoRe	69.78	45.17	84.96	60.66	63.57	90.10	79.52	62.61	21.14	32.94	61.04
CLIP-ViT-B/16 [†]	67.44	44.27	88.25	65.48	65.13	93.35	83.65	62.59	23.67	42.01	63.58
Caption Ensemble	61.39	36.05	60.59	44.84	51.69	85.40	71.64	49.61	49.61	33.32	51.48
CALIP	67.64	44.44	87.82	65.80	64.05	93.27	82.76	62.52	24.12	42.27	63.47
TPT [†]	68.98	47.75	87.79	66.87	68.04	94.16	84.67	65.50	24.78	42.44	65.10
X-MoRe	71.65	47.36	87.61	67.35	66.56	93.91	84.54	65.32	25.74	45.81	65.57

Table 1: Zero-shot performance across image classification benchmark datasets. We consistently used 16 captions for caption ensemble or X-MoRe. [†] performances are from Shu et al. (2022).

Method	ImageNet	ImageNet-A	ImageNet-V2	ImageNet-R	ImageNet-Sketch	Avg.	Variants Avg.
CLIP-RN50 [†]	58.16	21.83	51.41	56.15	33.37	44.18	40.69
Caption Ensemble	47.21	21.47	39.26	46.06	28.85	36.57	33.91
CALIP	58.21	21.67	51.44	55.96	33.30	44.12	40.59
TPT [†]	60.74	26.67	54.70	59.11	35.09	47.26	43.89
X-MoRe	62.71	26.49	55.25	62.21	40.41	49.41	46.09
CLIP-ViT-B/16 [†]	66.73	47.87	60.86	73.98	46.09	59.11	57.20
Caption Ensemble	47.11	22.62	39.64	47.84	29.34	37.31	34.86
CALIP	66.74	47.76	60.76	73.99	46.12	59.07	57.16
TPT [†]	68.98	54.77	63.45	77.06	47.94	62.44	60.81
X-MoRe	67.01	46.56	59.87	73.60	46.61	58.73	56.66

Table 2: Zero-shot performance on ImageNet and its variants. We consistently used 16 captions for caption ensemble or X-MoRe. [†] performances are from Shu et al. (2022).

for classification. Our baseline comparisons include both tuning-free inference (e.g., pre-trained CLIP P_{img} (Radford et al. 2021), an ensemble of retrieved captions P_{txt} ($K=16$), and CALIP (Guo et al. 2023)) and tuning-based inference (e.g., TPT (Shu et al. 2022)).

For the cross-modal retrieval in X-MoRe, we utilize laion-400m (Schuhmann et al. 2021) public dataset as an external image-text dataset. In the image-based retrieval step, we use visual embeddings extracted from an image encoder of CLIP-ViT-B/32, provided by the CLIP retrieval website¹. In the text-based fine-retrieval step, we use CLIP-ViT-L/14, discussed in Section 5.2. Across all experiments, we establish a pool of 128 image-text candidates, and subsequently, fine-retrieve 16 captions (i.e., N is 128 and K is 16), unless otherwise specified. We repeat experiments three times on different seeds.

4.2 Zero-shot Classification

Datasets We evaluate zero-shot ability across 10 image classification datasets: Caltech101 (Fei-Fei, Fergus, and Perona 2004), OxfordPets (Parkhi et al. 2012), StanfordCars (Krause et al. 2013), Flowers102 (Nilsback and Zisserman 2008), Food101 (Bossard, Guillaumin, and Van Gool 2014), FGVCAircraft (Maji et al. 2013), SUN397 (Xiao et al. 2010), DTD (Cimpoi et al. 2014), EuroSAT (Helber et al.

2019), and UCF101 (Soomro, Zamir, and Shah 2012). These datasets cover a wide spectrum of tasks, including generic object, scene, action, and fine-grained classification, along with specialized tasks such as texture recognition and satellite image analysis.

Results Table 1 provides the zero-shot performance results across 10 datasets. X-MoRe demonstrates the highest average accuracy in comparison to the baseline methods, even including a tuning-based inference approach (i.e., TPT). Specifically, for CLIP-RN50, our method consistently enhances the zero-shot performance across all datasets. It is notable that caption ensemble displays the lowest accuracy, implying the importance of ensemble with the image modality. This observation also highlights the effectiveness of X-MoRe’s balanced utilization of both modalities.

4.3 Domain Generalization

Datasets For the evaluation of general domain generalization, ImageNet (Deng et al. 2009) is used as the source dataset and four variants of ImageNet are used as the target datasets (i.e., ImageNetV2 (Recht et al. 2019), ImageNet-Sketch (Wang et al. 2019), ImageNet-A (Hendrycks et al. 2021b) and ImageNet-R (Hendrycks et al. 2021a)). However, our method and the baselines are not directly linked to the training approach. Thus, we adhere to the zero-shot evaluation protocol. In detail, ImageNetV2 is a recreated

¹<https://github.com/rom1504/clip-retrieval>

test set obtained from various sources using the same data collection process as ImageNet. ImageNet-Sketch contains sketches of the same 1,000 classes found in ImageNet. Meanwhile, ImageNet-A and ImageNet-R consist of 200 classes, a subset of ImageNet’s 1,000 classes. ImageNet-A comprises real-world images that have been adversarially filtered, causing current ImageNet classifiers to perform poorly. ImageNet-R presents ImageNet classes in diverse visual styles like paintings, cartoons, and sculptures.

Results Table 2 provides the performance evaluation on ImageNet and its variants. For CLIP-RN50, similar to zero-shot classification experiment, X-MoRe outperforms all other baselines, including the tuning-based inference approach. In fact, our approach can be viewed as an ensemble of ‘CLIP-RN50’ and ‘Caption Ensemble’ with modal-confidences, leading to performance enhancement. In other words, when the two modalities have comparable performance, our method offers significant performance improvement. However, for CLIP-ViT-B/16, our method decreases the performance. We speculate that, based on the results of large gap between ‘CLIP-ViT-B/16’ and ‘Caption Ensemble,’ our approach encounters challenges when one modality exhibits significant underperformance.

5 Ablation Study

In this section, we delve into ablation studies to provide further evidence for the effectiveness of our approach.

5.1 Importance of Text-based Fine-retrieval

We compare indirect and direct text retrieval to highlight the significance of text-based fine-retrieval. Indirect text retrieval indicates the process of searching K corresponding texts through image-based retrieval. Table 3 demonstrates that directly searching by measuring the similarity between a query image X and texts within a shared co-embedding space (i.e., text-based fine-retrieval in our algorithm) is one of the key factors.

Approach	Flower102	Caltech101
Indirect	65.04	88.92
Direct (Ours)	69.87	90.10

Table 3: Performance of zero-shot classification whether text retrieval is direct or not. CLIP-RN50 is used for inference.

5.2 Encoders for Text-based Fine-retrieval

The retrieval stage is intentionally structured to be distinct from inference to leverage the capabilities of improved language-image pre-trained models for cross-modal retrieval, as mentioned in Section 3.2. Specifically, for the text-based fine-retrieval, we can have the flexibility to scale the encoder. Table 4 reveals that using the largest image encoder with a smaller patch size enhances the retrieval quality, resulting in performance improvement. Therefore, CLIP-ViT-L/14 is used for our fine-retrieval.

Image Encoder	Flower102	Caltech101
ViT-B/32	64.84	88.88
ViT-B/16	66.46	89.21
ViT-L/14	69.87	90.10

Table 4: Performance of zero-shot classification according to the image encoder for the text-based fine-retrieval. CLIP-RN50 is used for inference.

5.3 Number of Retrieved Captions

Figure 4 illustrates the averaged zero-shot classification performance of X-MoRe across 10 datasets, varying the number of retrieved captions (i.e., K). The left and right figures depict the performance of CLIP-RN50 and CLIP-ViT-B/16, respectively. It is observed that the highest performance is achieved with 16 captions. This indicates that using an adequate number of retrieved texts is one of the key factors in achieving improved performance.

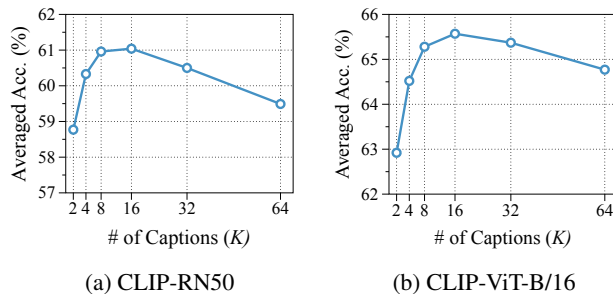


Figure 4: Averaged accuracy across 10 datasets according to the number of retrieved captions K .

5.4 Modal-confidence-based Ensemble

Lastly, we examine the importance of modal-confidence-based ensemble. The adjusted modal-confidence values (i.e., $\hat{\alpha}_{img}^t$ and $\hat{\alpha}_{txt}^t$) approach 1, if these modalities are reliable. To assess this, we compare our approach with the equal-confidence strategy. This strategy assumes that the two modalities always have the same reliability (i.e., $\hat{\alpha}_{img}^t = \hat{\alpha}_{txt}^t = 1$). Table 5 demonstrates that our modal-confidence-based ensemble slightly improves the performance in comparison to the straightforward equal-confidence-based ensemble.

Approach	Flower102	Caltech101	Cars	EuroSAT
Equal-conf.	69.63	90.10	60.41	32.18
Modal-conf.	69.87	91.15	60.65	32.94

Table 5: Performance of zero-shot classification whether the confidences of two modalities are equal (Equal-conf.) or not (Modal-conf.). CLIP-RN50 is used for inference.

Modality	Flower102	DTD	Pets	Cars	UCF101	Caltech101	Food101	SUN397	Aircraft	EuroSAT
Image	1.37	1.88	0.64	1.57	1.52	0.69	1.00	1.77	2.91	1.75
Text ($K=1$)	0.32	1.08	0.57	0.52	0.68	0.40	0.29	1.10	1.99	1.32
Text ($K=8$)	0.96	1.73	1.16	1.34	1.35	0.68	0.82	1.74	2.53	1.79
Text ($K=16$)	1.16	1.87	1.30	1.52	1.53	0.73	1.01	1.89	2.64	1.85
Text ($K=64$)	1.75	2.18	1.62	2.00	1.87	0.91	1.54	2.23	2.86	1.94

Table 6: Average of entropy of image-modal probability $P_{img}(y|X)$ and text-modal probability $P_{txt}(y|RC(X))$ according to the number of retrieved texts across 10 datasets.

6 Analysis

In this section, we present analyses related to confidences from the image-modal and text-modal perspectives.

6.1 Text Modality Has Lower Entropy than Image Modality

To examine the characteristics of the image-modal probability P_{img} and text-modal probability P_{txt} , we analyze their entropy distributions. Table 6 presents the average entropy values of P_{img} and P_{txt} according to the number of retrieved texts. Notably, when only one text is retrieved (i.e., $K=1$), the text modality exhibits significantly lower entropy compared to the image modality. This indicates that the text modality tends to be more overconfident in its predictions compared to the image modality. This phenomenon might be attributed to the shared text encoder between retrieved captions and text labels, where retrieved captions sometimes directly include the text labels.

Therefore, in alignment with a previous study (Lakshminarayanan, Pritzel, and Blundell 2017), we use multiple captions to prevent overconfident incorrect predictions. It is confirmed that the entropy of the text modality increases as the number of retrieved captions increases. When K is equal to 16, the average entropy becomes most similar between the two modalities, coinciding with the best performance of X-MoRe, shown in Section 5.3.

6.2 Confidences Should Be Adjusted

The different entropy distributions between the two modalities, as described in Section 6.1, leads to the different confidence distributions between the two modalities. For instance, while image-modal confidence α_{img} might range from 0.4 to 0.6, the text-modal confidence α_{txt} might range from 0.7 to 0.9. This distortion consistently makes the text modality more trustworthy. Moreover, although the average confidences are similar, a per-sample confidences can differ during test time t . To address this issue, we introduced an independent min-max adjustment for each modality. We compare the zero-shot performance between using modal-confidence without adjustment (i.e., α_{img}^t and α_{txt}^t) and with adjustment (i.e., $\hat{\alpha}_{img}^t$ and $\hat{\alpha}_{txt}^t$). Table 7 demonstrates the necessity of such independent confidence adjustment.

6.3 Correct Modality Has Higher Confidence

Finally, to examine whether modal-confidence is effectively adjusted, we divide the results into three cases according to the correctness of the predictions of $(P_{img}, P_{txt}, P_{ens})$: (1)

Confidence	Flower102	Caltech101	Cars	EuroSAT
$(\alpha_{img}^t, \alpha_{txt}^t)$	69.67	90.10	60.58	32.04
$(\hat{\alpha}_{img}^t, \hat{\alpha}_{txt}^t)$	69.87	91.15	60.66	32.94

Table 7: Performance of zero-shot classification according to the confidence adjustment.

(correct, incorrect, correct), (2) (incorrect, correct, correct), and (3) (incorrect, incorrect, correct).

Table 8 presents the average of $\hat{\alpha}_{img}/\hat{\alpha}_{txt}$ over all test samples for the three scenarios. A value greater than 1 indicates that the ensemble results prioritize the image modality over the text modality, while a value less than 1 indicates the ensemble results prioritize the text modality over the image modality. As we expected, the image modality is more influential than the text modality when P_{img} is correct and P_{txt} is wrong (i.e., case(1)), and vice versa (i.e., case(2)). Furthermore, the last case (i.e., case(3)) shows that the two modalities have similar power when both are crucial for correct prediction than using single modality.

Case	Flower102	Caltech101	Cars	EuroSAT
(1)	1.32	1.36	1.31	2.12
(2)	0.81	0.79	0.82	0.70
(3)	0.93	0.84	0.92	0.90

Table 8: Average of $\hat{\alpha}_{img}/\hat{\alpha}_{txt}$ over all test samples for the three scenarios.

7 Conclusion

In this paper, we propose X-MoRe, a cross-modal retrieval based inference method that maximizes CLIP’s zero-shot capabilities from both image and text modalities. Our method involves two key steps: *cross-modal retrieval* and *modal-confidence-based ensemble*. The former includes a coarse level of image-based retrieval which acquires image-text pairs from an external dataset and a finer level of text-based retrieval which directly considers texts given a query image. The latter step involves a probability ensemble between the two modalities, weighted by independent modal-confidence. While our work is currently constrained to scenarios with accessible external datasets, we believe that our approach contributes to the advancement of large-scale multi-modal models.

References

- Baek, J.; Aji, A. F.; and Saffari, A. 2023. Knowledge-Augmented Language Model Prompting for Zero-Shot Knowledge Graph Question Answering. *arXiv preprint arXiv:2306.04136*.
- Bossard, L.; Guillaumin, M.; and Van Gool, L. 2014. Food-101—mining discriminative components with random forests. In *Computer Vision—ECCV 2014: 13th European Conference, Zurich, Switzerland, September 6–12, 2014, Proceedings, Part VI 13*, 446–461. Springer.
- Chen, T.; Kornblith, S.; Norouzi, M.; and Hinton, G. 2020. A simple framework for contrastive learning of visual representations. In *International conference on machine learning*, 1597–1607. PMLR.
- Chen, Z.; Chen, G. H.; Diao, S.; Wan, X.; and Wang, B. 2023. On the Difference of BERT-style and CLIP-style Text Encoders. *arXiv preprint arXiv:2306.03678*.
- Cimpoi, M.; Maji, S.; Kokkinos, I.; Mohamed, S.; and Vedaldi, A. 2014. Describing textures in the wild. In *Proceedings of the IEEE conference on computer vision and pattern recognition*, 3606–3613.
- Deng, J.; Dong, W.; Socher, R.; Li, L.-J.; Li, K.; and Fei-Fei, L. 2009. Imagenet: A large-scale hierarchical image database. In *2009 IEEE conference on computer vision and pattern recognition*, 248–255. Ieee.
- Dosovitskiy, A.; Beyer, L.; Kolesnikov, A.; Weissenborn, D.; Zhai, X.; Unterthiner, T.; Dehghani, M.; Minderer, M.; Heigold, G.; Gelly, S.; et al. 2020. An image is worth 16x16 words: Transformers for image recognition at scale. *arXiv preprint arXiv:2010.11929*.
- Fei-Fei, L.; Fergus, R.; and Perona, P. 2004. Learning generative visual models from few training examples: An incremental bayesian approach tested on 101 object categories. In *2004 conference on computer vision and pattern recognition workshop*, 178–178. IEEE.
- Gao, Y.; Shi, X.; Zhu, Y.; Wang, H.; Tang, Z.; Zhou, X.; Li, M.; and Metaxas, D. N. 2022. Visual prompt tuning for test-time domain adaptation. *arXiv preprint arXiv:2210.04831*.
- Guo, Z.; Zhang, R.; Qiu, L.; Ma, X.; Miao, X.; He, X.; and Cui, B. 2023. Calip: Zero-shot enhancement of clip with parameter-free attention. In *Proceedings of the AAAI Conference on Artificial Intelligence*, volume 37, 746–754.
- Guzhov, A.; Raue, F.; Hees, J.; and Dengel, A. 2022. Audioclip: Extending clip to image, text and audio. In *ICASSP 2022-2022 IEEE International Conference on Acoustics, Speech and Signal Processing (ICASSP)*, 976–980. IEEE.
- He, K.; Chen, X.; Xie, S.; Li, Y.; Dollár, P.; and Girshick, R. 2022. Masked autoencoders are scalable vision learners. In *Proceedings of the IEEE/CVF conference on computer vision and pattern recognition*, 16000–16009.
- He, K.; Zhang, X.; Ren, S.; and Sun, J. 2016. Deep residual learning for image recognition. In *Proceedings of the IEEE conference on computer vision and pattern recognition*, 770–778.
- Helber, P.; Bischke, B.; Dengel, A.; and Borth, D. 2019. Eurosat: A novel dataset and deep learning benchmark for land use and land cover classification. *IEEE Journal of Selected Topics in Applied Earth Observations and Remote Sensing*, 12(7): 2217–2226.
- Hendrycks, D.; Basart, S.; Mu, N.; Kadavath, S.; Wang, F.; Dorundo, E.; Desai, R.; Zhu, T.; Parajuli, S.; Guo, M.; Song, D.; Steinhardt, J.; and Gilmer, J. 2021a. The Many Faces of Robustness: A Critical Analysis of Out-of-Distribution Generalization. *ICCV*.
- Hendrycks, D.; Zhao, K.; Basart, S.; Steinhardt, J.; and Song, D. 2021b. Natural adversarial examples. In *Proceedings of the IEEE/CVF Conference on Computer Vision and Pattern Recognition*, 15262–15271.
- Hu, Z.; Iscen, A.; Sun, C.; Wang, Z.; Chang, K.-W.; Sun, Y.; Schmid, C.; Ross, D. A.; and Fathi, A. 2023. Reveal: Retrieval-augmented visual-language pre-training with multi-source multimodal knowledge memory. In *Proceedings of the IEEE/CVF Conference on Computer Vision and Pattern Recognition*, 23369–23379.
- Iscen, A.; Caron, M.; Fathi, A.; and Schmid, C. 2023. Retrieval-Enhanced Contrastive Vision-Text Models. *arXiv preprint arXiv:2306.07196*.
- Iscen, A.; Fathi, A.; and Schmid, C. 2023. Improving image recognition by retrieving from web-scale image-text data. In *Proceedings of the IEEE/CVF Conference on Computer Vision and Pattern Recognition*, 19295–19304.
- Kang, M.; Baek, J.; and Hwang, S. J. 2022. KALA: knowledge-augmented language model adaptation. *arXiv preprint arXiv:2204.10555*.
- Kang, M.; Kwak, J. M.; Baek, J.; and Hwang, S. J. 2023. Knowledge Graph-Augmented Language Models for Knowledge-Grounded Dialogue Generation. *arXiv preprint arXiv:2305.18846*.
- Khandelwal, U.; Levy, O.; Jurafsky, D.; Zettlemoyer, L.; and Lewis, M. 2019. Generalization through memorization: Nearest neighbor language models. *arXiv preprint arXiv:1911.00172*.
- Kim, G.; Kwon, T.; and Ye, J. C. 2022. Diffusionclip: Text-guided diffusion models for robust image manipulation. In *Proceedings of the IEEE/CVF Conference on Computer Vision and Pattern Recognition*, 2426–2435.
- Krause, J.; Stark, M.; Deng, J.; and Fei-Fei, L. 2013. 3d object representations for fine-grained categorization. In *Proceedings of the IEEE international conference on computer vision workshops*, 554–561.
- Lakshminarayanan, B.; Pritzel, A.; and Blundell, C. 2017. Simple and scalable predictive uncertainty estimation using deep ensembles. *Advances in neural information processing systems*, 30.
- Lei, J.; Berg, T. L.; and Bansal, M. 2021. mtvr: Multilingual moment retrieval in videos. *arXiv preprint arXiv:2108.00061*.
- Li, X. L.; and Liang, P. 2021. Prefix-tuning: Optimizing continuous prompts for generation. *arXiv preprint arXiv:2101.00190*.

- Li, Y.; Fan, H.; Hu, R.; Feichtenhofer, C.; and He, K. 2023. Scaling language-image pre-training via masking. In *Proceedings of the IEEE/CVF Conference on Computer Vision and Pattern Recognition*, 23390–23400.
- Liu, J.; Yu, T.; Peng, H.; Sun, M.; and Li, P. 2022. Cross-lingual cross-modal consolidation for effective multilingual video corpus moment retrieval. In *Findings of the Association for Computational Linguistics: NAACL 2022*, 1854–1862.
- Maji, S.; Rahtu, E.; Kannala, J.; Blaschko, M.; and Vedaldi, A. 2013. Fine-grained visual classification of aircraft. *arXiv preprint arXiv:1306.5151*.
- Menon, S.; and Vondrick, C. 2022. Visual classification via description from large language models. *arXiv preprint arXiv:2210.07183*.
- Nilsback, M.-E.; and Zisserman, A. 2008. Automated flower classification over a large number of classes. In *2008 Sixth Indian conference on computer vision, graphics & image processing*, 722–729. IEEE.
- Parkhi, O. M.; Vedaldi, A.; Zisserman, A.; and Jawahar, C. 2012. Cats and dogs. In *2012 IEEE conference on computer vision and pattern recognition*, 3498–3505. IEEE.
- Radford, A.; Kim, J. W.; Hallacy, C.; Ramesh, A.; Goh, G.; Agarwal, S.; Sastry, G.; Askell, A.; Mishkin, P.; Clark, J.; et al. 2021. Learning transferable visual models from natural language supervision. In *International conference on machine learning*, 8748–8763. PMLR.
- Recht, B.; Roelofs, R.; Schmidt, L.; and Shankar, V. 2019. Do imagenet classifiers generalize to imagenet? In *International conference on machine learning*, 5389–5400. PMLR.
- Schuhmann, C.; Vencu, R.; Beaumont, R.; Kaczmarczyk, R.; Mullis, C.; Katta, A.; Coombes, T.; Jitsev, J.; and Komatsuzaki, A. 2021. Laion-400m: Open dataset of clip-filtered 400 million image-text pairs. *arXiv preprint arXiv:2111.02114*.
- Shu, M.; Nie, W.; Huang, D.-A.; Yu, Z.; Goldstein, T.; Anandkumar, A.; and Xiao, C. 2022. Test-time prompt tuning for zero-shot generalization in vision-language models. *Advances in Neural Information Processing Systems*, 35: 14274–14289.
- Soomro, K.; Zamir, A. R.; and Shah, M. 2012. UCF101: A dataset of 101 human actions classes from videos in the wild. *arXiv preprint arXiv:1212.0402*.
- Vaswani, A.; Shazeer, N.; Parmar, N.; Uszkoreit, J.; Jones, L.; Gomez, A. N.; Kaiser, Ł.; and Polosukhin, I. 2017. Attention is all you need. *Advances in neural information processing systems*, 30.
- Wang, H.; Ge, S.; Lipton, Z.; and Xing, E. P. 2019. Learning Robust Global Representations by Penalizing Local Predictive Power. In *Advances in Neural Information Processing Systems*, 10506–10518.
- Xiao, J.; Hays, J.; Ehinger, K. A.; Oliva, A.; and Torralba, A. 2010. Sun database: Large-scale scene recognition from abbey to zoo. In *2010 IEEE computer society conference on computer vision and pattern recognition*, 3485–3492. IEEE.
- Xu, H.; Ghosh, G.; Huang, P.-Y.; Okhonko, D.; Aghajanyan, A.; Metze, F.; Zettlemoyer, L.; and Feichtenhofer, C. 2021. Videoclip: Contrastive pre-training for zero-shot video-text understanding. *arXiv preprint arXiv:2109.14084*.
- Zhang, R.; Fang, R.; Zhang, W.; Gao, P.; Li, K.; Dai, J.; Qiao, Y.; and Li, H. 2021. Tip-adapter: Training-free clip-adapter for better vision-language modeling. *arXiv preprint arXiv:2111.03930*.
- Zhou, K.; Yang, J.; Loy, C. C.; and Liu, Z. 2022a. Conditional prompt learning for vision-language models. In *Proceedings of the IEEE/CVF Conference on Computer Vision and Pattern Recognition*, 16816–16825.
- Zhou, K.; Yang, J.; Loy, C. C.; and Liu, Z. 2022b. Learning to prompt for vision-language models. *International Journal of Computer Vision*, 130(9): 2337–2348.